International Journal of Pharmaceutics 423 (2012) 37–44

Contents lists available at ScienceDirect

International Journal of Pharmaceutics

journal homepage: www.elsevier.com/locate/ijpharm

Study of serum interaction with a cationic nanoparticle: Implications for *in vitro* endocytosis, cytotoxicity and genotoxicity

Maysaloun Merhi[a,b,1], Christophe Youta Dombu[a,c,1], Alizée Brient[a,b], Jiang Chang[a,c], Anne Platel[a,b,d], Frank Le Curieux[a,b,d,2], Daniel Marzin[a,b,d], Fabrice Nesslany[b], Didier Betbeder[a,c,e,*]

[a] *Université Lille Nord de France, F-59000 Lille, France*
[b] *IPL, EA 4483, Laboratoire de Toxicologie, Institut Pasteur de Lille, 1 rue du Professeur Calmette, BP 245, 59019 Lille, France*
[c] *CHU Lille, EA 4483, IMPRT, IFR 114, Faculté de Médecine pôle recherche, Université de Lille 2, 59000 Lille, France*
[d] *UDSL, EA 4483, Département Toxicologie-Santé Publique-Environnement, Faculté de Pharmacie, 59000 Lille, France*
[e] *Université d'Artois, 9 rue du temple, 62030 Arras, France*

ARTICLE INFO

Article history:
Received 13 January 2011
Received in revised form 6 July 2011
Accepted 11 July 2011
Available online 22 July 2011

Keywords:
Cationic nanoparticles
Endocytosis
Genotoxicity
Human bronchial epithelial cells
Comet assay
Micronucleus test

ABSTRACT

We used well-characterized and positively charged nanoparticles (NP^+) to investigate the importance of cell culture conditions, specifically the presence of serum and proteins, on NP^+ physicochemical characteristics, and the consequences for their endocytosis and genotoxicity in bronchial epithelial cells (16HBE14o-). NP^+ surface charge was significantly reduced, proportionally to NP^+/serum and NP^+/BSA ratios, while NP^+ size was not modified. Microscopy studies showed high endocytosis of NP^+ in 16HBE14o-, and serum/proteins impaired this internalization in a dose-dependent manner. Toxicity studies showed no cytotoxicity, even for very high doses of NP^+. No genotoxicity was observed with classic comet assay while primary oxidative DNA damage was observed when using the lesion-specific repair enzyme, formamidopyrimidine DNA-glycosylase (FPG). The micronucleus test showed NP^+ genotoxicity only for very high doses that cannot be attained *in vivo*. The low toxicity of these NP^+ might be explained by their high exocytosis from 16HBE14o- cells. Our results confirm the importance of serum and proteins on nanoparticles endocytosis and genotoxicity.

1. Introduction

Understanding the potential risks associated with human exposure to nanoparticles (NPs) is a major public health concern which has intensified with the increasing manufacturing and the wider use of NPs, inevitably leading to potentially greater exposure of humans to NPs. In the field of nanomedicine, NPs are currently being investigated for numerous applications, including diagnostic, drug delivery, vaccines, medical imaging, nanoarrays, implants and prostheses (Couvreur and Vauthier, 2006; Pinaud et al., 2006; Riehemann et al., 2009). It is therefore necessary to better understand the impact of such exposure in order to be aware of the potential risks for the human health and to ensure the appropriately controlled application of nanotechnologies. The airway route of exposure, extending from the oral and nasal cavities to the lungs, constitutes a very large area of potential interaction with airborne NPs. The airway epithelium nevertheless constitutes a highly regulated and impermeable barrier of tight junctions and this physical and physiological barrier effectively limits airborne NPs entry. However, both natural and manufactured NPs have been reported to be able to cross this barrier by strongly interacting with airway epithelial cells (Kreyling et al., 2009), though the details of the mechanisms involved remain poorly understood. According to some authors, exposure to NPs was related to toxic effects in the lungs such as chronic obstructive pulmonary diseases (Fanizza et al., 2007), fibrosis, oxidative stress and inflammation, genotoxicity and mutagenesis (Shvedova et al., 2009), as well as toxicity in distal organs (Oberdorster et al., 2005). However, these toxic effects probably related to their high surface reactivity were observed at very high doses of NPs. Other studies have shown that, at high concentrations and in the presence of serum, NPs form large aggregates which are unlikely to reach the deeper lungs (Oberdorster, 2010).

Owing largely to the great diversity of NPs in the environment, encompassing a wide range of different characteristics and physicochemical properties, it is difficult to reliably predict the intrinsic toxicity of NPs in general. Each NP can indeed be described by a set of physicochemical properties (*i.e.*, size, surface charge, shape,

* Corresponding author at: CHU Lille, EA 4483, IMPRT, IFR 114, Faculté de Médecine pôle recherche, Université de Lille 2, 59000 Lille, France.
Tel.: +33 320 62 68 83.
E-mail addresses: didier.betbeder@univ-lille2.fr, didier.betbeder@neuf.fr (D. Betbeder).
[1] These authors have equal contributions to the manuscript.
[2] Present address: European Chemicals Agency, Annankatu 18, FIN-00121 Helsinki, Finland.

0378-5173/$ – see front matter © 2011 Elsevier B.V. All rights reserved.
doi:10.1016/j.ijpharm.2011.07.014

aggregation and composition, etc.), all likely to influence their fate and actions in the human airway (Yang et al., 2009). Therefore, assessing the importance of each parameter is a key step toward understanding their potential toxicity. Another difficulty in studying the toxicity of NPs is the lack of widely accepted methods and relevant models. Because of some of the specific properties of NPs, it is thought that current *in vitro* toxicity assays validated for "common" chemicals could be inappropriate for studying NPs (Kroll et al., 2009). Finally, most of the toxicity studies published to date have focused on the investigation of cytotoxic effects and have overlooked the more subtle cellular alterations, such as genotoxicity (Singh et al., 2009), which might contribute to human health risks posed by NPs.

Here we present results from a study of a 60 nm cationic NP (NP^+) which can be used at high concentrations without aggregation in the presence or absence of serum proteins. *In vitro* studies are performed in absence of mucus, therefore increasing nanoparticles contact with cells for evaluating their potential toxicity. The aim of our work was to investigate the importance of cell culture conditions, specifically the presence of serum and proteins in the culture media, on the physicochemical characteristics of NP^+ (size and zeta potential), and the consequences on this NP^+ endocytosis and genotoxicity in a human bronchial epithelial cell line (16HBE14o-). For genotoxicity testing, we used the comet assay (primary DNA damage) and the micronucleus test (chromosomal aberration assay).

2. Methods

2.1. Reagents and chemicals

The reagents and chemicals used in the experiments were purchased from the following suppliers: maltodextrin from Roquette (Roquette, France); glycidyl-trimethyl-ammonium chloride (GTMA), minimum essential media (MEM), foetal calf serum (FCS), phosphate buffered saline (PBS) and DAPI from GIBCO Invitrogen SARL, Cergy-Pontoise, France; giemsa reagent, penicillin, streptomycin, mitomycin C (MMC, CAS No. 50-07-7), methyl methanesulfonate (MMS, CAS No. 66-27-3), cytochalasin B, Triton X-100, EDTA, trizma base, hepes, RNase, propidium iodide, 5-[4,6-dichlorotriazin-2-yl] amino fluorescein isothiocyanate (FITC), epichlorhydrin (1-chloro-2,3-epoxypropane), KCl, NaCl and bovine serum albumin (BSA) from Sigma–Aldrich, Saint-Quentin Fallavier, France; methanol from Panreac Quimica, Barcelona, Spain; trypsin from Biochrom AG, Berlin, Germany; normal melting point and low melting point agaroses from Biorad, Marnes la Coquette, France; repair endonuclease formamidopyrimidine glycosylase (Fpg) from New England Bio-Labs via Ozyme, Saint-Quentin en Yvelines, France; acetic acid from VWR, Fontenay-sous-bois, France; DMSO from Acros Organics, Noisy le Grand, France; $NaBH_4$ from Acros Organics, Noisy-le-Grand, France; NaOH, Na_2HPO_4 and absolute ethanol from Merck, Darmstadt, Germany.

2.2. Nanoparticles

2.2.1. Preparation of polysaccharide cationic nanoparticles from maltodextrin and characterization

Polysaccharide cationic NPs (NP^+) were prepared from maltodextrin as described previously (Major et al., 1997; Paillard et al., 2010). Briefly, 100 g of maltodextrin was dissolved in 2 N sodium hydroxide with magnetic stirring at room temperature. Addition to the crude mixture of epichlorhydrin and glycidyl-trimethyl-ammonium chloride (hydroxycholine, cationic ligand) yielded cationic polysaccharide gel. The gel was then neutralized with acetic acid and crushed with a high pressure homogenizer (Emulsiflex C3, France). The NP^+ obtained were purified by tangential flow ultra-filtration (Centramate Minimum II, PALL, France) using a 300 kDa membrane (PALL, France) to remove oligosaccharides, low-molecular weight reagents and salts. Whenever necessary, NP^+ labeling was achieved by covalently binding fluorescein isothiocyanate (FITC) to the polysaccharide core (Prieur et al., 1996). These labeled particles were washed and purified by tangential flow ultra-filtration (Centramate Minimum II, PALL, France) using a 100 kDa membrane (PALL, France) with demineralised water until no free marker was detected in the ultra-filtrate. All NP^+ solutions were stored in sterile tubes after filtration through a 0.2-μm filter. We also checked the stability of FITC-NP^+ labeling and confirmed that no free FITC was released from NP^+ after storage for 6 months at 4 °C: moreover, the labeling was stable after 24 h incubation at 37 °C in complete medium or in PBS.

2.2.2. Protein loading to NP^+

BSA was loaded onto nanoparticles by mixing NP^+ (original concentration = 5 mg/ml) and BSA (original concentration = 1 mg/ml) in PBS for 10 min at room temperature, under stirring, using different ratios of NP^+/BSA (*i.e.*, 1/0.3; 1/1; 1/3 and 1/5 (w/w)). In these conditions the loading was quantitative as assessed by Paillard et al. (2010).

2.2.3. Size and zeta potential analysis

The average hydrodynamic diameter and the zeta potential of NP^+ were measured in 15 mM NaCl, using the Malvern nanoZS (Malvern Instruments, France). The analyses were performed in triplicate. In order to determine the size and the zeta potential in presence of serum, the NP^+ were first diluted in MEM containing different concentrations of FCS (0%, 2.5%, 5% and 10% (v/v)).

2.3. Cell line and culture conditions

The human bronchial epithelial cell line 16HBE14o- was obtained from Dr. Gruenert D.C. (Colchester, Vermont, USA) and their doubling time was assessed as approximately 22 h (data not shown).

2.3.1. Endocytosis study

The cells were seeded on 8-well glass chamber slides (LabTek® II, Thermo Scientific Nunc Lab, UK) at a density of 3×10^5 cells/well (0.8 cm^2). Chamber slides were first coated with a mixture of collagen and fibronectin (4/1 (v/v)). Cells were incubated until confluence at 37 °C in a humidified 5% CO_2 atmosphere. The cell culture medium (MEM supplemented with 10% decomplemented FCS, 100 U/ml penicillin, 100 μg/ml streptomycin and 1% L-glutamine) was renewed every 2 days. After 4 days in culture, the cells were confluent with a density of approximately 1×10^6 cells/well (0.8 cm^2).

2.3.2. Genotoxicity assessment

16HBE14o- cells were maintained at 37 °C in a humidified 5% CO_2 atmosphere in MEM growth medium supplemented with 200 U/ml penicillin, 50 μg/ml streptomycin and 10% of decomplemented FCS. Cells were seeded at a density of 4×10^5 cells/well (3 ml culture medium/well) in 6-well cell culture plates (9.6 cm^2; Falcon™, Becton Dickinson Biosciences, France) and incubated for 22 h prior to exposure to the NP^+ in order to allow exponential cell growth and maximum cell attachment.

2.4. Confocal microscopy analysis

Cells were washed twice with PBS and incubated with 10 μg of NP^+ (corresponding to approximately 12.5 μg of NP^+ for 1 cm^2 of cells) in 0.4 ml PBS for 30 min at 37 °C, then washed twice with PBS.

Cells were fixed with 200 μl of 4% paraformaldehyde for 10 min at room temperature, then washed twice with PBS and incubated for 10 min with 80 μL of DAPI (1/1000^e (v/v) diluted in demineralised water). The slide-attached monolayer cells were photographed under confocal microscope (Leica, Wetzlar, Germany). Endocytosis was visualized by confocal microscopy; pictures represent slices taken every 3 μm from the luminal to the abluminal side (1–10). All experiments were performed in quadruplet and four pictures of each condition were taken in different fields of the slides (about 100 cells per field). Fluorescence intensity of each picture was measured using the software SigmaScan Pro 5 (Systat software, Inc., Point Richmond, CA, USA). Calculations were performed using the statistical software program GraphPad Prism 5 (GraphPad Softwares, Inc., La Jolla, CA, USA). For statistical analyses we used a one-way analysis of variance (ANOVA) and Student's *t*-test. The results were considered significant when $p < 0.05$.

2.5. Genotoxicity assays (comet assay and micronucleus test)

2.5.1. Cell treatment

NP^+ were dispersed in PBS at the highest initial concentration of 50 mg/ml. Successive suspensions were then made in PBS in order to obtain the following concentrations: 25, 12.5, 6.25, 3.125 and 1.5625 mg/ml. All the NP^+ suspensions were vortexed for 2 min and sonicated for 10 min at room temperature (Ultrasonic water bath, 550 W, Advantage lab GmbH, Belgium). Each concentration was then diluted at 10% in the culture medium (MEM with or without 10% FCS) giving the final NP^+ concentrations used for cell treatment of: 5000, 2500, 1250, 625, 312.5 and 156.25 μg/ml (corresponding to 2604, 1302, 651, 326, 163 and 81 μg/cm^2).

In order to determine if serum influenced NP^+ behaviour, two types of treatment were carried out: cells were incubated for 3 h with the NP^+ dispersed either in serum-free MEM medium or in MEM supplemented with 10% FCS. Positive controls (mitomycine C (MMC) 2.5 μg/ml and methyl methanesulphonate (MMS) 20 μg/ml) were included in the micronucleus test and comet assay, respectively. Negative control was PBS diluted at 10% in the culture medium (MEM with or without 10% FCS). After the treatment, the cells were washed twice with PBS and immediately harvested (for the comet assay) or incubated in complete medium (MEM + 10% FCS) for 40 h before harvesting (for the micronucleus test). Each treatment was coupled to an assessment of cytotoxicity as described below.

2.5.2. Assessment of cytotoxicity

For the comet assay, cytotoxicity was first assessed at harvest using the trypan blue dye exclusion assay. Viable cells appeared refringent and dead cells incorporated trypan blue (0.4%). Cells were observed and scored using a Malassez hemacytometer. Results were expressed as percent of cell survival, *i.e.*, the percent ratio of viable (unstained) cells in treated *versus* control groups. Concentrations which led to more than 70% of viability were submitted to a genotoxicity assessment.

Cytotoxicity was also evaluated by performing the halo assay as described by Sestili et al. (2006). Indeed, it has been shown that alkaline-halo assay (AHA) may be more sensitive than the comet assay in detecting apoptotic and necrotic processes (Bacso and Eliason, 2001).

For the micronucleus test, cytotoxicity was evaluated by calculating the percentage of relative population doubling (RPD), where population doubling = [log (post-treatment cell number/initial cell number)]/log (2), as recommended by OECD guidance (OECD guidance, 2010). NP^+ concentrations leading to a RPD of more than $55 \pm 5\%$ were considered as of low or no cytotoxicity, and were submitted to genotoxicity assessment.

2.5.3. Assessment of genotoxicity

2.5.3.1. Comet assay protocol. The comet assay was performed under alkaline conditions (pH > 13) as described by Singh et al. (1988). Slight modifications were employed in order to detect specifically the oxidative DNA damage, based on Collins' procedures (Collins et al., 1993). Formamidopyrimidine glycosylase (Fpg) was used to detect oxidative DNA base damage, as recommended by the European Standards Committee on Oxidative DNA damage (ESCODD, 2003).

At the end of the treatment, 2.10^4 cells from each well were mixed with 75 μl of 0.5% low-melting point agarose kept at 37 °C before rapidly transferring onto pre-coated slides (two layers of normal agarose (1.5% and 0.8%)). Five slides were prepared for each dose: 2 slides treated with Fpg (Fpg (+)), 2 slides without Fpg (Fpg (−)), and 1 slide corresponding to the halo assay. All the following steps were sheltered from daylight to prevent the occurrence of additional DNA damage.

Fpg (−) and Fpg (+) slides were immersed for at least 1 h at 4 °C in a cold lysing solution (2.5 M NaCl, 100 mM EDTA, 10 mM Trizma Base, pH 10, supplemented with 1% Triton X-100 and 10% DMSO). After lysis, slides were washed and equilibrated for 2×5 min in enzyme buffer (40 mM HEPES, 100 mM KCl, 0.5 mM EDTA, 0.2 mg/ml BSA; pH 8). Fpg (−) slides were washed immediately in water; Fpg (+) slides received 75 μl of Fpg solution (0.6 U Fpg/slide) and coverslips, and were incubated at 37 °C for 35 min. At the end of this enzymatic step, slides were quickly rinsed with cold PBS.

All the slides were then placed in a horizontal gel electrophoresis tank previously filled with fresh electrophoresis solution (1 mM EDTA and 300 mM NaOH, pH > 13) for 20 min to allow DNA unwinding and expression of single-strand breaks and alkali-labile sites. Next, electrophoresis was performed for 20 min using an electric current of 20 V and 25 mA. Slides were then placed for 2×5 min in neutralization solution (0.4 M Trizma base, pH 7.5) and gels were dehydrated by immersion in absolute ethanol for 5 min. Finally, slides were air-dried and stored at room temperature.

2.5.3.2. Cells scoring in the comet assay. Slides were coded and analysed blind. We added 25 μl of propidium iodide solution (20 μg/ml in distilled water) and a coverslip on each slide. Slides were then examined at 250× magnification using a fluorescence microscope (Leica Microscopy and Scientific Instruments Group, Heerbrugg, Switzerland) equipped with an excitation filter of 515–560 nm and a 590 nm barrier filter, connected through a gated CCD camera to Comet Image Analysis System software, version 4.0 (Perceptive Instruments Ltd., Haverhill, United Kingdom).

We scored 100 randomly selected cells per test condition (50 cells from each of the two replicate slides). The olive tail moment (OTM), recommended by Olive et al. (1990), was used to evaluate DNA damage. OTM is calculated as a product of two factors: the percentage of DNA in the tail (% tail DNA) and the distance between the intensity centroids (centres of gravity) of the head and the tail along the *x*-axis of the comet.

In the halo assays, 100 randomly selected cells per slide were analysed and manually enumerated using a counter.

2.5.3.3. In vitro micronucleus test (MNT). At the end of the recovery period (40 h), 16HBE14o- cells were collected by trypsinization, washed with MEM, transferred to 15 ml polypropylene tubes and centrifuged at 165 G for 6 min. Cells were then treated for 4 min with a hypotonic solution (MEM diluted 1:1 (v/v) in distilled water, 10 ml/tube). At the end of the hypotonic shock, a pre-fixation step was performed by adding 1 ml/tube of cold Carnoy I mixture (methanol/acetic acid, 3:1 (v/v)). Cells were then centrifuged and fixed with 10 ml of cold Carnoy I for at least 10 min at room temperature. After another centrifugation, cells were spread on glass

slides, air-dried at room temperature (at least over-night), stained for 10 min with 4% Giemsa water solution, rinsed with distilled water and dried at room temperature. For each concentration, 2 slides were prepared for analysis.

The slides were finally coded and analysed blind. Micronuclei (MN), identified according to criteria recommended by Fenech et al. (2003), were scored at 500× magnification in 1000 intact mononuclear cells per slide. For each concentration, the frequency of MN was obtained for 2000 mononuclear cells.

2.5.4. Statistical analysis

The OTM frequencies did not follow a Gaussian distribution (Bauer et al., 1998). Thus, the non-parametric Mann–Whitney *U*-test was used to evaluate the statistical difference between groups (*i.e.*, each dose) and the difference between each dose *versus* the negative control in the Comet assay. Differences with a $p < 0.05$ were considered statistically significant. All statistical analyses were performed with StatView® Software (version 5.0, SAS Institute Inc., SAS Campus Drive, Cary, NC 27513, USA).

For the micronucleus test, the statistical significance of difference between groups was determined using the CHI^2-test. Differences with a $p < 0.05$ were considered statistically significant.

3. Results

3.1. Characterization of NP+

The size of the NP+ was measured by dynamic light scattering and their zeta potential measured using the Malvern nanoZS. The mean diameter of the NP+ was 64 ± 13 nm, with a polydispersity index (PdI) value of 0.22 and their mean zeta potential was +25 ± 1.5 mV. They were also found to be spherical by transmission electron microscopy (Dombu et al., 2010). NP+ size and zeta potential analyses were performed in order to investigate the impact of serum on these parameters and to check if the assays were actually performed on NP+ at their nanoscale form rather than on aggregates and/or agglomerates of NP+ (Figs. 1 and 2). As observed in Fig. 1A, for a constant amount of NP+, the zeta potential gradually decreased when FCS concentration was increased in the medium. In addition, at the concentration of 1250 μg/ml of NP+, the zeta potential of NP+ was reduced by up to 50% when FCS concentration was increased from 0% to 10% in the medium. Interestingly, when similar measurements were performed using 5000 μg/ml of NP+, the zeta potential remained unchanged even at a maximum FCS concentration of 10%. These results strongly suggest that, rather than the presence of FCS in the medium, it is mostly the ratio NP+/FCS which modulates the zeta potential of NP+. Similar results were observed when different amounts of BSA were associated with NP+ (Fig. 1B), and a sharp decrease in zeta potential was observed when NP+/BSA ratio decreased. Interestingly, the measurements of NP+ size performed under these conditions showed that neither serum nor BSA significantly modified the size of the NP+ (Fig. 2), even at the highest amounts of serum or BSA tested.

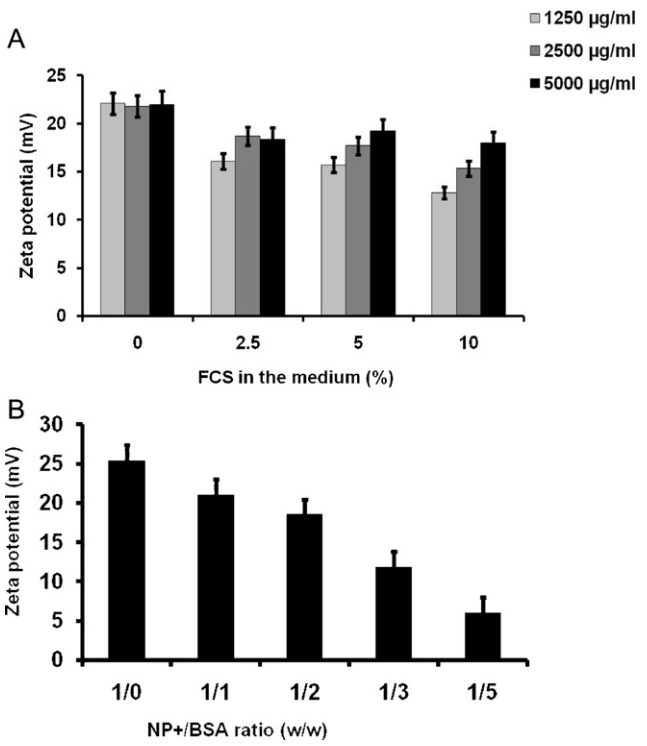

Fig. 1. Analysis of NP+ zeta potential in presence of FCS and BSA. NP+ (5000, 2500 and 1250 μg/ml) were diluted in MEM medium containing FCS at different concentrations (0%, 2.5%, 5% or 10%) (A), or diluted at 1 mg/mL in 15 mM NaCl containing different amounts of BSA (w/w) (B). Experiments were performed in triplicate and the mean values are represented on the graph. Error bars represent the standard deviations between triplicate analyses with the NanoZetasizer.

3.2. Effect of serum and proteins on NP+ endocytosis

We investigated the ability of NP+ to be endocytosed by 16HBE14o- cells. Fig. 3 shows confocal microscopy slices of cells after 30 min incubation with NP+. As observed, NP+ were endocytosed by cells and found in cytoplasm as punctuated forms, characterizing an endosomal uptake.

We studied the influence of serum and BSA on NP+ endocytosis (Fig. 4). The endocytosis of NP+ in presence of 10% FCS was significantly reduced in both PBS and MEM (respectively 60% and 40% decrease), suggesting that FCS partially inhibited the endocytosis of NP+ (Fig. 4A). Similar results were obtained when NP+ were associated with BSA (major protein of serum) (Fig. 4B), and 40% inhibition of NP+ endocytosis was observed with an NP+/BSA ratio of 1/5 (w/w). Moreover, this reduction seemed to be directly dependent on the NP+/BSA ratio, as endocytosis decreased proportionally with the BSA increase. These results show that the presence of serum or proteins in the culture medium can significantly reduce NP+ endocytosis.

3.3. Cytotoxicity studies

NP+ did not induce significant cytotoxic effects in these cells up to the highest tested concentration of 2604 μg/cm^2 as assessed by the trypan blue dye exclusion assay (data not shown). Indeed, whatever the test conditions, no indication of an increase in apoptotic or necrotic cells was noted using the halo assay. In fact, our results showed roughly 4% of necrotic cells and 1% of apoptotic cells for both the treated concentrations and controls (Table 1).

3.4. Comet assay

Both standard and Fpg modified tests were performed in presence or in absence of serum. In the absence of Fpg none of the OTM values was statistically significantly different either with or without serum (Fig. 5A). When Fpg was added, statistically significant increases in DNA damage were observed without serum at the dose of 81, 163 and 1302 μg/cm^2 (Fig. 5B). When serum was added during the treatment, OTM values described a bell shape curve, with a significant increase in DNA damage at 163, 236 and 2604 μg/cm^2. In addition, a statistically significant effect of serum on the toxicity of NP was observed at 81, 163 and 1302 μg/cm^2.

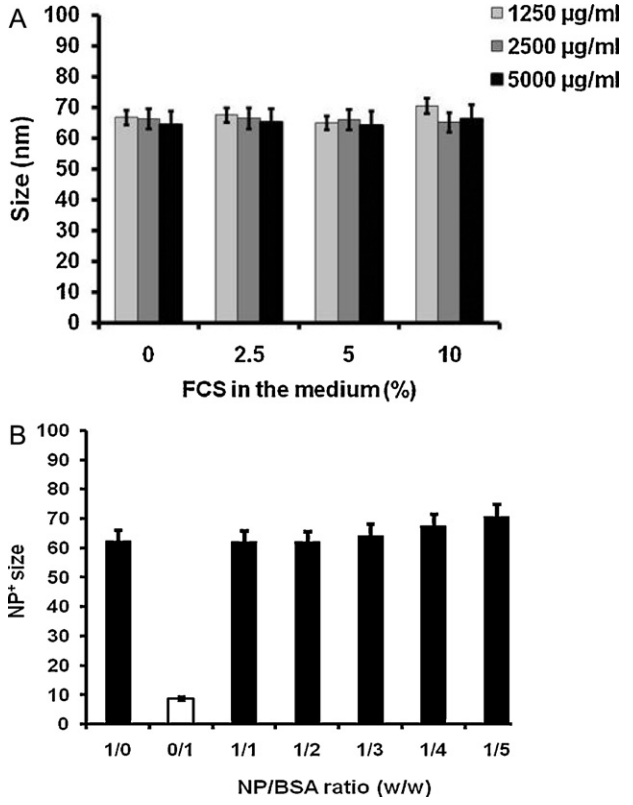

Fig. 2. Measurements of NP^+ size in presence of FCS and BSA. Size analysis of different concentrations (5000, 2500, 1250 μg/mL) of NP^+ diluted in MEM medium containing 0%, 2.5%, 5% or 10% FCS (A); (B): 1000 μg/ml NP^+ diluted in PBS containing different amounts of BSA (w/w). Experiments were performed in triplicate and the mean values are represented on the graph. Error bars represent the standard deviations between triplicate analyses with the NanoZetasizer.

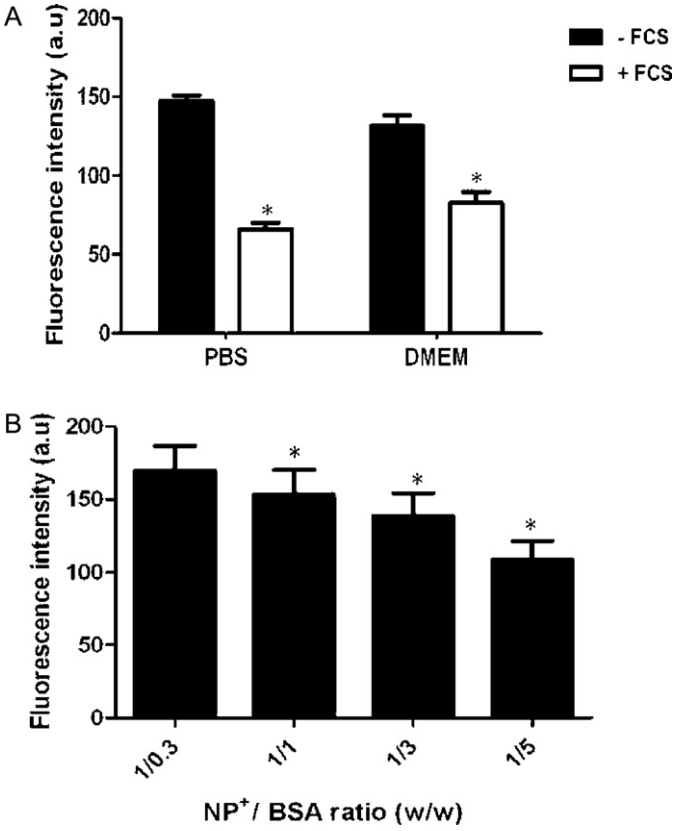

Fig. 4. Quantification of NP^+ endocytosis. Cells were incubated 30 min at 37 °C with 10 μg of FITC labeled NP^+ (corresponds to 12.5 μg/cm^2), associated with BSA at the ratios indicated, then washed twice with PBS and fixed for 10 min at room temperature with 4% PFA. Internalized NP^+ was observed under confocal microscopy and endocytosis was evaluated by measuring fluorescence intensities under each condition. Experiments were performed in triplicate and the mean values (and standard deviations) are represented on the graph.

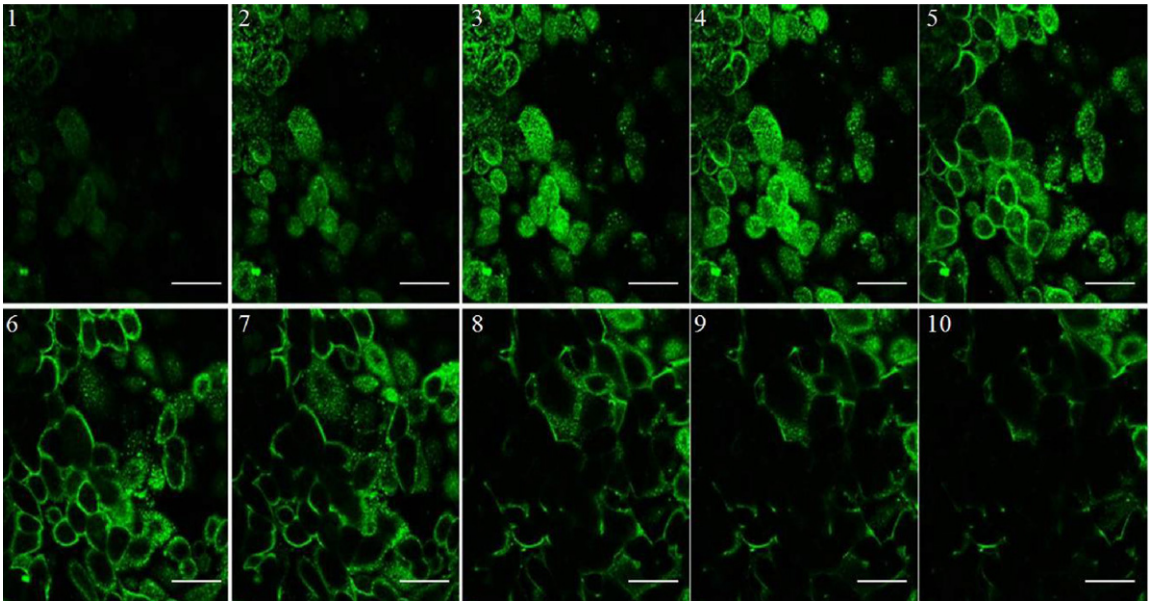

Fig. 3. Study of NP^+ uptake by confocal microscopy. Cells were incubated 30 min at 37 °C with 10 μg of FITC labeled NP^+ (12.5 μg/cm^2), they were washed twice with PBS and fixed for 10 min at room temperature with 4% PFA. Endocytosis was visualized by confocal microscopy; pictures represent slices taken every 3 μm from the luminal to the abluminal side (1–10). Scale bar 50 μm.

Table 1
Halo assay in 16HBE14o-: percentage of necrotic and apoptotic cells at different concentrations of NP^+ and in the presence or not of serum (FCS(+) and (−)).

NP^+ [μg/cm²]	FCS (+)		FCS (−)	
	Necrotic cells	Apoptotic cells	Necrotic cells	Apoptotic cells
0	0	0	0	0
81	0	0	1	0
163	0	0	0	0
326	1	0	3	0
651	0	1	0	0
1302	1	0	2	1
2604	0	0	4	0

3.5. *In vitro* micronucleus test

The MNT was used to assess the induction of chromosomal aberrations after exposure to the NP^+. The tested concentrations led to RPD values ≥55 ± 5% and were considered as of low or no cytotoxicity (data not shown). The frequency of micronucleated cells in 1000 mononuclear cells in Giemsa-stained specimens is shown in Fig. 6. We observed significant increases in MN formation when cells were treated at concentrations >326 μg/cm² either in presence or not of FCS.

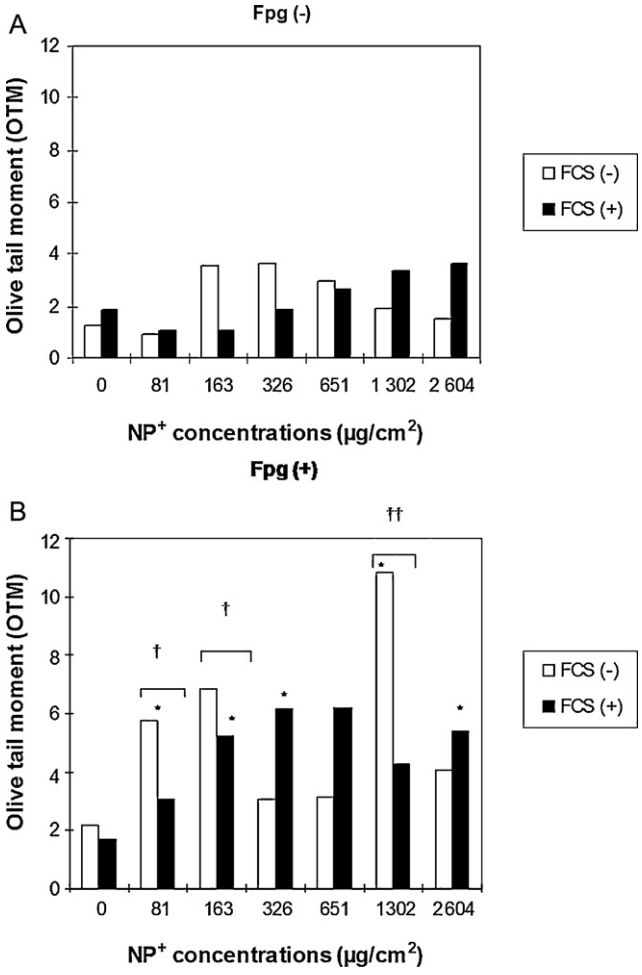

Fig. 5. DNA damage on 16HBE14o- cells treated by NP^+ in MEM (complemented or not by FCS). Median OTM values are presented for the classic and modified comet assays (a and b, respectively). Mann–Whitney test was used for statistical comparison of OTM values between the treatments (with or without FCS; $^{\dagger}p < 0.05$; $^{\dagger\dagger}p < 0.001$) and for each dose *versus* negative control ($^{*}p < 0.05$).

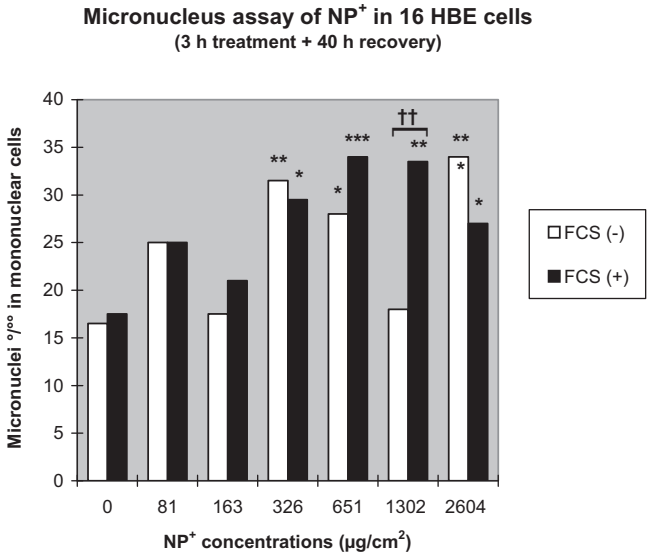

Fig. 6. Micronucleus test of NP^+ in 16HBE14o- cells. 16HBE14o- cells were treated for 3 h under increasing concentrations of NP^+ added to MEM in the presence or absence of FCS. Positive control was mitomycin C (2.5 μg/ml) and negative control consisted of cells treated with the vehicle (PBS). After a recovery period of 40 h the micronucleus test was performed as described in Section 2. Micronuclei (MN) were scored at 500× magnification for 2000 mononuclear cells in each concentration. MN frequency is expressed for 1000 mononuclear cells. CHI_2 test was used for statistical comparison of the micronuclei°/°° in treated *versus* control cells; $^{*}p < 0.05$; $^{**}p < 0.01$; $^{***}p < 0.001$, and between each treatment condition (with or without FCS); $^{\dagger\dagger}p < 0.01$.

4. Discussion

Nanoparticles can be described by their physicochemical properties (size, surface charge, shape, aggregation and composition), all of which are likely to have an influence on their fate and behaviour in the human airway (Yang et al., 2009). Understanding the role of NPs' physicochemical properties in their interactions with airway epithelial cells is a key step in evaluating its eventual toxicity to people exposed via inhalation. Therefore it is necessary to develop specific *in vitro* models that take into account NPs physicochemical properties and to study their toxicity in a manner relevant to potential exposure conditions (Gul et al., 2009).

Numerous studies have shown that several types of particles form aggregates when diluted in culture medium. For example, Hackenberg et al. (2010) showed that 15–30 nm titanium dioxide (TiO_2) NPs had a strong tendency to aggregate in aqueous solution and formed micro-sized complexes up to a size of 285 nm (and in a few cases 2 μm), in spite of intense sonication of the suspensions. Similar observations were made in our laboratory with SiO_2 and TiO_2 NPs in PBS (data not shown). Such aggregations can significantly modify the experimental outcome by leading to a heterogenic population of nano- and microparticles with different physicochemical characteristics and behaviours from that of the NPs at their nanoscale. The size of NPs in suspension seems to be a key parameter as most of the published studies so far started with NPs but ended up studying aggregates which are not only expected to be different in their interactions with cells, but are not expected to reach the deep into the lungs once inhaled (Lamprecht et al., 2001).

In the present study, we tested a 60 nm polysaccharide cationic NP (NP^+), the composition, size, shape and surface charge of which are well characterized and controllable. The aim of this work was to investigate the importance of cell culture conditions, specifically the presence of serum and proteins in the culture media on the physicochemical characteristics of NP^+ and also to establish the conditions under which the NP^+ could be studied purely in their nanoscale form in order to assess their endocytosis and

genotoxicity. For this purpose, we used the human bronchial epithelial cell line 16HBE14o- (Cozens et al., 1994). These cells are highly similar to the primary bronchial epithelium, which make them suitable for mechanistic studies of bronchial epithelium, including transport regulation (Ehrhardt et al., 2003), drug delivery (Forbes, 2000) and toxicology studies (Hussain et al., 2009).

Studies performed *in vivo* have demonstrated the ability of these cationic NP^+ to efficiently deliver proteins after sublingual or nasal administration (Debin et al., 2002; El mir et al., 2001; Razafindratsita et al., 2007). We recently described that these NP^+ were endocytosed via the clathrin pathway and were highly exocytosed by human epithelial airway via a cholesterol dependent pathway (Dombu et al., 2010). Despite the increasing number of studies performed on NPs administered via the airway (*e.g.*, Roy and Vij, 2010), their potential genotoxicity remains poorly investigated. A more complete understanding of NPs' toxicity is a prerequisite for further preclinical development and eventual use in humans. However, to date, there is no validated or widely accepted model to assess this issue. In the present study, we have tried to better define an experimental approach for the *in vitro* study of cationic NPs (NP^+) cytotoxicity and genotoxicity by examining the implications of cell culture conditions on their endocytosis, cytotoxicity and genotoxicity to a human bronchial cell line.

4.1. Effect of FCS and BSA interactions on NP^+ size, surface charge and endocytosis

NPs for nanomedicine applications should be tested in the presence of proteins, particularly in the light of recent findings that the interaction of proteins with NPs modifies NPs size, size distribution and zeta potential (Rausch et al., 2010). Proteins such as albumin, IgG, IgA, IgM, alpha 1-acid glycoprotein, alpha 1-antitrypsin, alpha 2-macroglobulin, transferrin, haptoglobin, and coeruloplasmin are highly present not only in cell culture medium but also in physiological air mucosa (Szabó et al., 1980). We first investigated the effect of FCS and BSA on NP^+ size and surface charge. Neither FCS nor BSA modified NP^+ size at any of the concentrations tested, even with a NP^+/BSA ratio of 1/5 (w/w). In addition, we observed that FBS did not modify NP^+ endocytosis pathway (data not shown). However, we observed that FCS and BSA can sharply reduce NP^+ surface charge and that this reduction was proportional to NP^+/FCS and NP^+/BSA ratios. These results might be explained by associations between the cationic surface charges of NP^+ and anionic serum compounds such as BSA. Similar results have previously been described by Ehrenberg et al. (2009), who showed that polystyrene NPs immersed in culture medium were quickly coated by serum proteins with maximum coating occurring in a matter of seconds to minutes. These results suggest that studies performed using NPs should be performed at low concentration.

We were also interested in investigating the ability of NP^+ to penetrate 16HBE14o- cells. Our results showed that NP^+ were endocytosed after 30 min of incubation, as demonstrated by confocal microscopy studies, but that their endocytosis was greatly reduced in the presence of FCS or BSA. Moreover, pre-incubation of the NP^+ with BSA in PBS prior to the endocytosis study also reduced their endocytosis and this inhibition was correlated with the NP^+/BSA ratio during incubation. As the endocytosis mechanisms were not modified, this reduced endocytosis could be explained by the decrease in nanoparticle surface charge due to protein adsorption (Osaka et al., 2009).

Interestingly, cytotoxicity studies showed that these NP^+ were not cytotoxic even at the highest dose tested, a result that might be explained by the high level of NP^+ exocytosis observed (Dombu et al., 2010).

4.2. Comet assay interpretation

In the present study, the comet assay was used both for its sensitivity in assessing DNA damage and for its usefulness as a first approach in understanding the NP^+ mechanisms of action. In addition, the realisation of a modified assay using the enzyme Fpg, enables to both increase the specificity and sensitivity of the assay by making detectable a wide range of damage (such as 8-oxo-dG, AP-sites, oxidized purines and pyrimidines, etc.) not detected in the classic comet assay.

The results obtained without Fpg did not show any statistically significant increase in DNA damage compared to the negative control over the range of NP^+ doses tested in the current study, with or without the addition of serum (+/− FCS). In parallel, when Fpg was used, our results showed higher, statistically significant median OTM values and the presence of serum partially decreased this effect. This could be explained by the reduced endocytosis of the NP^+ observed in presence of serum. These results tend to indicate that using Fpg permitted the identification of oxidative damage in the absence of FCS. However, since these effects were not clearly dose-related, it may be that they were caused by different phenomena. One hypothesis is that damage observed at high NP^+ doses may be related to other damage such as lipid peroxidation or the formation of MDA, 4-HNE. It is noteworthy that these DNA lesions were probably not induced by secondary apoptotic or necrotic phenomenon, considering the negative results obtained with the halo assay. On the other hand, a different trend was observed when serum was added to culture medium: a bell-shaped response curve was observed with the first statistically significant OTM value at 163 $\mu g/cm^2$. It is interesting to note that serum had an effect on the response of 16HBE14o- cells.

Our findings confirm the results obtained in some studies which suggested that various nanoparticles are able to induce oxidative stress. It has been reported that nanoparticles may generate ROS and this mechanism is thought to play a major role in their observed cytotoxic and genotoxic effects and in addition that nanoparticles could indirectly induce oxidative stress by disturbing the balance between oxidant and anti-oxidant processes such as the glutathione system (Stone et al., 1998). Furthermore, some studies have suggested that nanoparticles may activate intracellular pathways, also leading to ROS generation (*e.g.*, synthesis of pro-inflammatory cytokines and chemokines) (Oberdorster et al., 2005). Nevertheless, the precise mechanisms activated by nanoparticles to induce ROS generation and cytotoxicity remain unknown.

4.3. Micronucleus test results interpretation

Preliminary assays showed that significant and prohibitive mortality was repeatedly observed when 16HBE14o- cells were exposed to cytochalasin B (CytoB) (data not shown). Thus, all following assays were carried out without CytoB. Significant increases in the number of micronuclei in 16HBE14o- cells were observed in presence or absence of FCS. These effects may be explained by the generation of ROS that induce lipid adducts and cells membrane degradation which could not be observed after a 3-h treatment (as used in the comet assay), but that appeared only after 40 h of recovery (applied in the micronucleus test). Finally, the increase in the number of micronuclei at concentrations that did not show primary DNA damage in the comet assay may be related to secondary mechanisms leading to indirect alterations of the mitotic apparatus. However, the results obtained in the presence of FCS showed that the lowest genotoxic effect was detected at 326 $\mu g/cm^2$ (MNT). These concentrations correspond to a deposition of 0.456 kg of nanoparticles in the lungs, respectively, assuming that the lungs' absorptive surface is about 140 m^2 (Sakagami, 2006), the epithelial

cells are under mitosis, and that all the NPs crossed the mucus barrier and stay in contact with cells for hours, and such exposures are considered to be unrealistic.

5. Conclusion

Results revealed the importance of cell culture conditions on NP^+ physicochemical characteristics, uptake and genotoxicity on 16HBE14o- cells. Toxicity studies showed that, even at very high concentrations, the studied NP^+ were neither cytotoxic nor genotoxic as measured by the classical comet assay. The use of Fpg-modified comet assay allowed the observance of primary DNA damage that is normally repaired by the cells. This modified assay showed that primary damage occurred but that the presence of serum partially protected the cells, possibly by lowering NP^+ uptake by cells. In addition, the micronucleus test showed that NP^+ were genotoxic at high doses. The low observed toxicity observed of these cationic nanoparticles could be explained by their high exocytosis that lowers cell burden. These results confirm the importance of fully characterizing nanoparticles' behaviour under different cell culture conditions and confirm the role of serum protein on nanoparticles' interaction with, and genotoxicity toward cells.

Acknowledgments

This work was supported by the grants from Institut de Recherche en Environnement Industriel (IRENI) and the Conseil Régional du Nord-Pas-de-Calais. The authors would also like to thank Mike Howsam for the critical reading of the manuscript.

References

Bacso, Z., Eliason, J.F., 2001. Measurement of DNA damage associated with apoptosis by laser scanning cytometry. Cytometry 45, 180–186.
Bauer, E., Recknagel, R.D., Fiedler, U., Wollweber, L., Bock, C., Greulich, K.O., 1998. The distribution of the tail moments in single cell gel electrophoresis (comet assay) obeys a chi-square (chi^2) not a gaussian distribution. Mutat. Res. 398, 101–110.
Collins, A.R., Duthie, S.J., Dobson, V.L., 1993. Direct enzymic detection of endogenous oxidative base damage in human lymphocyte DNA. Carcinogenesis 14, 1733–1735.
Couvreur, P., Vauthier, C., 2006. Nanotechnology: intelligent design to treat complex disease. Pharm. Res. 23, 1417–1450.
Cozens, A.L., Yezzi, M.J., Kunzelmann, K., Ohrui, T., Chin, L., Eng, K., Finkbeiner, W.E., Widdicombe, J.H., Gruenert, D.C., 1994. CFTR expression and chloride secretion in polarized immortal human bronchial epithelial cells. Am. J. Respir. Cell Mol. Biol. 10, 38–47.
Debin, A., Kravtzoff, R., Santiago, J.V., Cazales, L., Sperandio, S., Melber, K., Janowicz, Z., Betbeder, D., Moynier, M., 2002. Intranasal immunization with recombinant antigens associated with new cationic particles induces strong mucosal as well as systemic antibody and CTL responses. Vaccine 20, 2752–2763.
Dombu, C.Y., Kroubi, M., Zibouche, R., Matran, R., Betbeder, D., 2010. Characterization of endocytosis and exocytosis of cationic nanoparticles in airway epithelium cells. Nanotechnology 21, 355102.
Ehrenberg, M.S., Friedman, A.E., Finkelstein, J.N., Oberdorster, G., McGrath, J.L., 2009. The influence of protein adsorption on nanoparticle association with cultured endothelial cells. Biomaterials 30, 603–610.
Ehrhardt, C., Kneuer, C., Laue, M., Schaefer, U.F., Kim, K.J., Lehr, C.M., 2003. 16HBE14o- human bronchial epithelial cell layers express P-glycoprotein, lung resistance-related protein, and caveolin-1. Pharm. Res. 20, 545–551.
El mir, S., Casanova, A., Betbeder, D., Triebel, F., 2001. A combination of interleukin-2 and 60 nm cationic supramolecular biovectors for the treatment of established tumours by subcutaneous or intranasal administration. Eur. J. Cancer 37, 1053–1060.
ESCODD, European Standards Committee on Oxidative DNA Damage, 2003. Measurement of DNA oxidation in human cells by chromatographic and enzymic methods. Free Radic. Biol. Med. 34, 1089–1099.
Fanizza, C., Ursini, C.L., Paba, E., Ciervo, A., Di Francesco, A., Maiello, R., De Simone, P., Cavallo, D., 2007. Cytotoxicity and DNA-damage in human lung epithelial cells exposed to respirable alpha-quartz. Toxicol. In Vitro 21, 586–594.
Fenech, M., Chang, W.P., Kirsch-Volders, M., Holland, N., Bonassi, S., Zeiger, E., 2003. HUMN project: detailed description of the scoring criteria for the cytokinesis-block micronucleus assay using isolated human lymphocyte cultures. Mutat. Res. 534, 65–75.
Forbes, B., 2000. Human airway epithelial cell lines for in vitro drug transport and metabolism studies. Pharm. Sci. Technol. Today 3, 18–27.
Gul, M.O., Jones, S.A., Dailey, L.A., Nacer, H., Ma, Y., Sadouki, F., Hider, R., Araman, A., Forbes, B., 2009. A poly(vinyl alcohol) nanoparticle platform for kinetic studies of inhaled particles. Inhal. Toxicol. 21, 631–640.
Hackenberg, S., Friehs, G., Froelich, K., Ginzkey, C., Koehler, C., Scherzed, A., Burghartz, M., Hagen, R., Kleinsasser, N., 2010. Intracellular distribution, geno- and cytotoxic effects of nanosized titanium dioxide particles in the anatase crystal phase on human nasal mucosa cells. Toxicol. Lett. 195, 9–14.
Hussain, S., Boland, S., Baeza-Squiban, A., Hamel, R., Thomassen, L.C., Martens, J.A., Billon-Galland, M.A., Fleury-Feith, J., Moisan, F., Pairon, J.C., Marano, F., 2009. Oxidative stress and proinflammatory effects of carbon black and titanium dioxide nanoparticles: role of particle surface area and internalized amount. Toxicology 260, 142–149.
Kreyling, W.G., Semmler-Behnke, M., Seitz, J., Scymczak, W., Wenk, A., Mayer, P., Takenaka, S., Oberdorster, G., 2009. Size dependence of the translocation of inhaled iridium and carbon nanoparticle aggregates from the lung of rats to the blood and secondary target organs. Inhal. Toxicol. 21 (Suppl. 1), 55–60.
Kroll, A., Pillukat, M.H., Hahn, D., Schnekenburger, J., 2009. Current in vitro methods in nanoparticle risk assessment: limitations and challenges. Eur. J. Pharm. Biopharm. 72, 370–377.
Lamprecht, A., Schäfer, U., Lehr, C.M., 2001. Size-dependent bioadhesion of micro- and nanoparticulate carriers to the inflamed colonic mucosa. Pharm. Res. 18, 788–9318.
Major, M., Prieur, E., Tocanne, J.F., Betbeder, D., Sautereau, A.M., 1997. Characterization and phase behaviour of phospholipid bilayers adsorbed on spherical polysaccharidic nanoparticles. Biochim. Biophys. Acta 3, 2–40.
Oberdorster, G., Oberdorster, E., Oberdorster, J., 2005. Nanotoxicology: an emerging discipline evolving from studies of ultrafine particles. Environ. Health Perspect. 113, 823–839.
Oberdorster, G., 2010. Safety assessment for nanotechnology and nanomedicine: concepts of nanotoxicology. J. Intern. Med. 267, 89–105.
OECD, 2010. Guideline for the Testing of Chemicals, In Vitro Mammalian Cell Micronucleus Test Organization for Economic Co-operation and Development.
Olive, P.L., Banath, J.P., Durand, R.E., 1990. Heterogeneity in radiation-induced DNA damage and repair in tumor and normal cells measured using the comet assay. Radiat. Res. 122, 86–94.
Osaka, T., Nakanishi, T., Shanmugam, S., Takahama, S., Zhang, H., 2009. Effect of surface charge of magnetite nanoparticles on their internalization into breast cancer and umbilical vein endothelial cells. Colloids Surf. B: Biointerfaces 71, 325–333.
Paillard, A., Passirani, C., Saulnier, P., Kroubi, M., Garcion, E., Benoit, J.P., Betbeder, D., 2010. Positively-charged, porous, polysaccharide nanoparticles loaded with anionic molecules behave as 'stealth' cationic nanocarriers. Pharm. Res. 27, 126–133.
Pinaud, F., Michalet, X., Bentolila, L.A., Tsay, J.M., Doose, S., Li, J.J., Iyer, G., Weiss, S., 2006. Advances in fluorescence imaging with quantum dot bio-probes. Biomaterials 27, 1679–1687.
Prieur, E., Betbeder, D., Niedergang, F., Major, M., Alcover, A., Davignon, J.L., Davrinche, C., 1996. Combination of human cytomegalovirus recombinant immediate-early protein (IE1) with 80 nm cationic biovectors: protection from proteolysis and potentiation of presentation to CD4+ T-cell clones in vitro. Vaccine 14, 511–520.
Rausch, K., Reuter, A., Fischer, K., Schmidt, M., 2010. Evaluation of nanoparticle aggregation in human blood serum. Biomacromolecules 11, 2836–2839.
Razafindratsita, A., Saint-Lu, N., Mascarell, L., Berjont, N., Bardon, T., Betbeder, D., Van Overtvelt, L., Moingeon, P., 2007. Improvement of sublingual immunotherapy efficacy with a mucoadhesive allergen formulation. J. Allergy Clin. Immunol. 120, 278–285.
Riehemann, K., Schneider, S.W., Luger, T.A., Godin, B., Ferrari, M., Fuchs, H., 2009. Nanomedicine – challenge and perspectives. Angew. Chem. Int. Ed. Engl. 48, 872–897.
Roy, I., Vij, N., 2010. Nanodelivery in airway diseases: challenges and therapeutic applications. Nanomedicine 6, 237–244.
Sakagami, M., 2006. In vivo, in vitro and ex vivo models to assess pulmonary absorption and disposition of inhaled therapeutics for systemic delivery. Adv. Drug Deliv. Rev. 58, 1030–1060.
Sestili, P., Martinelli, C., Stocchi, V., 2006. The fast halo assay: an improved method to quantify genomic DNA strand breakage at the single-cell level. Mutat. Res. 607, 205–214.
Shvedova, A.A., Kisin, E.R., Porter, D., Schulte, P., Kagan, V.E., Fadeel, B., Castranova, V., 2009. Mechanisms of pulmonary toxicity and medical applications of carbon nanotubes: two faces of Janus? Pharmacol. Ther. 121, 192–204.
Singh, N., Manshian, B., Jenkins, G.J., Griffiths, S.M., Williams, P.M., Maffeis, T.G., Wright, C.J., Doa, S.H., 2009. Nanogenotoxicology: the DNA damaging potential of engineered nanomaterials. Biomaterials 30, 3891–3914.
Singh, N.P., McCoy, M.T., Tice, R.R., Schneider, E.L., 1988. A simple technique for quantitation of low levels of DNA damage in individual cells. Exp. Cell Res. 175, 184–191.
Stone, V., Shaw, J., Brown, D.M., Macnee, W., Faux, S.P., Donaldson, K., 1998. The role of oxidative stress in the prolonged inhibitory effect of ultrafine carbon black on epithelial cell function. Toxicol. In Vitro 12, 649–659.
Szabó, S., Barbu, Z., Lakatos, L., László, I., Szabó, A., 1980. Local production of proteins in normal human bronchial secretion. Respiration 39, 172–178.
Yang, H., Liu, C., Yang, D., Zhang, H., Xi, Z., 2009. Comparative study of cytotoxicity, oxidative stress and genotoxicity induced by four typical nanomaterials: the role of particle size, shape and composition. J. Appl. Toxicol. 29, 69–78.